Non-linear analysis of reinforced concrete sections under diffusion process and deterioration damage

Análisis no-lineal de secciones de hormigón armado bajo proceso de difusión y daño por deterioro

Jesús Miguel Bairán García[a], **Pablo Marín San Román**[b]

[a] Ph.D., M.Sc., Civil Engineer. Universitat Politècnica de Catalunya. Professor. jesus.miguel.bairan@upc.edu

[b] M.Sc. Civil Engineer. Arenas & Asociados. Structural Engineer. pmarin@arenasing.com

RESUMEN

El daño por corrosión es una de las principales causas de deterioro de las estructuras existentes de hormigón. En este artículo se presente un modelo no-lineal de secciones de fibras combinado con la simulación 2D de difusión de carbonatación o cloruros en el tiempo a partir de una distribución de concentraciones en la superficie. El modelo permite simular con el avance de la concentración crítica de los agentes y el inicio probable de la corrosión y la posterior evolución del daño en las fibras de acero y hormigón. Es posible así realizar un análisis detallado de la distribución del daño y los correspondientes efectos en la resistencia, rigidez y ductilidad.

ABSTRACT

Corrosion damage is one of the main causes of deterioration in existing concrete structures. This paper presents a non-linear fibre sectional model combined with a 2D simulation of the diffusion process of carbonation or chlorides along time, starting from the surface concentration distribution. The model allows the simulation of the evolution of the concentration of critical contents of the agents that trigger the corrosion initiation and the subsequent evolution of the damage in the concrete and steel fibres. This enables the detailed distribution of the corrosion damage in time and the corresponding effects in the strength, stiffness and ductility.

PALABRAS CLAVE: Corrosión, difusión, deterioro, modelo numérico, distribución daño, seguridad
KEYWORDS: Corrosion, diffusion, deterioration, numerical model, damage distribution, safety

1. Introduction

It is estimated that 3%-4% of the global GDP is expended per annum to restore deteriorated existing structures. In addition, the the budget for maintenance and rehabilitation of existing structures currently exceeds that of new constructions [1, 2] in many countries.

The significant economic and environmental impact of infrastructure replacement justifies the need for efficient resource management to ensure both safe and sustainable use these facilities. A sustainable approach consists on extending the service life of the existing facilities whenever possible. However, this requires adequate analytical tools are essential for realistically assess the need for repair of existing structures, optimized strengthening design or adapting them.

This paper presents an approach that leverages current computational capabilities and knowledge to develop a more general methodology. The model embeds a detailed diffusion and non-linear analysis at the model that relates environmental exposure and the temporal component of structural deterioration. A damage model is coupled to each local region of the section as function of the local damage produced in the reinforcement and concrete material points. This is further linked to a fibre sectional model to obtain the cross-section response at various time steps, including: (i) a loss of bearing capacity, (ii) a loss of stiffness, and (iii) a loss of ductility of the section. The capabilities of the developed model are demonstrated through an application example. Finally, conclusions and recommendations are drawn.

2. Mechanical analysis framework

The structural response at the cross-section level is simulated by means of a fibre discretization. This allows a general description of the arbitrary sectional geometry and material heterogeneity by discretizing materials points as fibres. Each fibre *i*, located in a coordinate (y_i, z_i) on the cross-section's plane, is assigned a finite area A_i and a material's constitutive equation $\sigma_i(\varepsilon_i)$. This approach is equivalent to the finite differences method, in which the vector of internal forces is integrated as shown in Eq. (1).

$$\boldsymbol{s_s} = \begin{bmatrix} N_x \\ M_y \\ M_z \end{bmatrix} = \sum_{i=1}^{n} \begin{bmatrix} 1 \\ z_i \\ -y_i \end{bmatrix} \sigma_i(\varepsilon_i) A_i \qquad (1)$$

Where N_x, M_y and M_z are the axial force and bending moments around the local axes of the section's plane. ε_i is the normal strain in fibre *i*, which is computed by means of the Navier-Bernoulli hypothesis, Eq. (2). ε_0, ϕ_y and ϕ_z the axial strain and curvature along the *y* and *z* axes of the frame element at the cross-section's point.

$$\varepsilon_i = \begin{bmatrix} 1 & z_i & -y_i \end{bmatrix} \begin{bmatrix} \varepsilon_0 \\ \phi_y \\ \phi_z \end{bmatrix} \qquad (2)$$

3. Diffusion problem and implementation

The diffusion model provides a robust numerical framework for simulating the transport of aggressive agents, such as chlorides, within concrete structures. The methodology is rooted in Fick's Laws of Diffusion, which mathematically describe the movement of particles driven by concentration gradients. The model aims to predict the spatiotemporal evolution of these agents and their impact on structural integrity.

The governing equation for the diffusion process is derived from Fick's 2nd Law:

$$D\nabla^2 c = \frac{\partial c}{\partial t} \qquad (3)$$

Where *c* represents the concentration and *D* the diffusion coefficient. These equations establish the relationship between the concentration gradient and its temporal evolution.

The model requires the definition of boundary conditions, such as fixed concentration (c_D) or flux (c_N), as well as initial conditions (c_0) specifying the starting distribution of the aggressive agent.

To solve the associated partial differential equation (PDE), the Finite Element Method (FEM) is employed. This method discretizes the spatial domain into finite elements and approximates the solution within each element.

The implementation follows a systematic approach:

1. Geometry Definition: The domain is discretized into finite elements, with nodal coordinates and connectivity matrices defining the geometry. In the problem at hand, the geometric domain represents the cross-section of the structural element, including the reinforcement bars, concrete and distribution of relevant materials properties. Specific to the diffusion problem, the distribution of the diffusion coefficient is described along the geometry.

2. Matrix Assembly: Element-level contributions are computed and assembled into global matrices defining and algebraic system of equation.

In this implementation, a weak-form of Eq. (3) is used, which reduces the order of integration of the right-hand term of Eq. (3), i.e. the divergence term, resulting in the weak integral form shown in Eq. (4). Where $\boldsymbol{N}$ is the vector of shape functions.

3. Condition Application: Initial and boundary conditions are incorporated into the system of equations.

4. Time Advancement: The time-dependent variation term ($\dot{\boldsymbol{c}}$) in Eq. (3) is solved in a step-by-step process using a finite-differences approach.

5. Postprocessing: Results, such as concentration profiles and their temporal evolution, are analyzed to assess structural implications.

$$-\int_{\Omega} \nabla\boldsymbol{N}\nabla\boldsymbol{N}^T\, d\Omega\boldsymbol{c} + \int_{\partial\Omega} \boldsymbol{N}\, d\Gamma\boldsymbol{c_N} = \int_{\Omega} \boldsymbol{N}\boldsymbol{N}^T\, d\Omega\dot{\boldsymbol{c}} \tag{4}$$

Fig. 1 shows the evolution of the ratio of the chloride concentration with respect to the critical value (C/C_0) for different cross-section geometries and irregular initial conditions. In particular, Fig. 1-above depicts the case of an I-shaped section with chloride initial distribution is applied in the bottom face, while Fig. 1-middle represents a T-shaped section with the initial concentration in the bottom corner. It is noticed that the model is capable of predicting the irregular distribution of the chloride ingress, which will translate into different affectation in the concrete and reinforcement along the section. On the other hand, Fig. 1-bottom shows a bridge box-section where the chloride attacks the upper face, a result of, for instance, use of de-icing salts.

4. Damage model

For a given concentration of carbonation or chloride computed in the previously describe diffusion analysis, material damage may be developed in both concrete and steel reinforcement.

The damage model serves as a critical component for evaluating the structural consequences of reinforcement corrosion in concrete. By linking the concentration of aggressive agents with the material degradation, the model quantifies the resulting changes in mechanical and geometric properties, enabling an accurate assessment of the structural response.

Corrosion of steel reinforcement is simulated representing the following effects:

1. Reduction of cross-sectional effective area: Corrosion reduces the effective reinforcement area, weakening the steel's load-carrying capacity.

2. **Material degradation:** Mechanical properties such as ductility and yield stress diminishes with the corrosion level.

3. Concrete cracking: The volumetric expansion of corrosion products induces tensile stresses in the surrounding concrete, leading to cracking and, in severe cases, spalling of the cover.

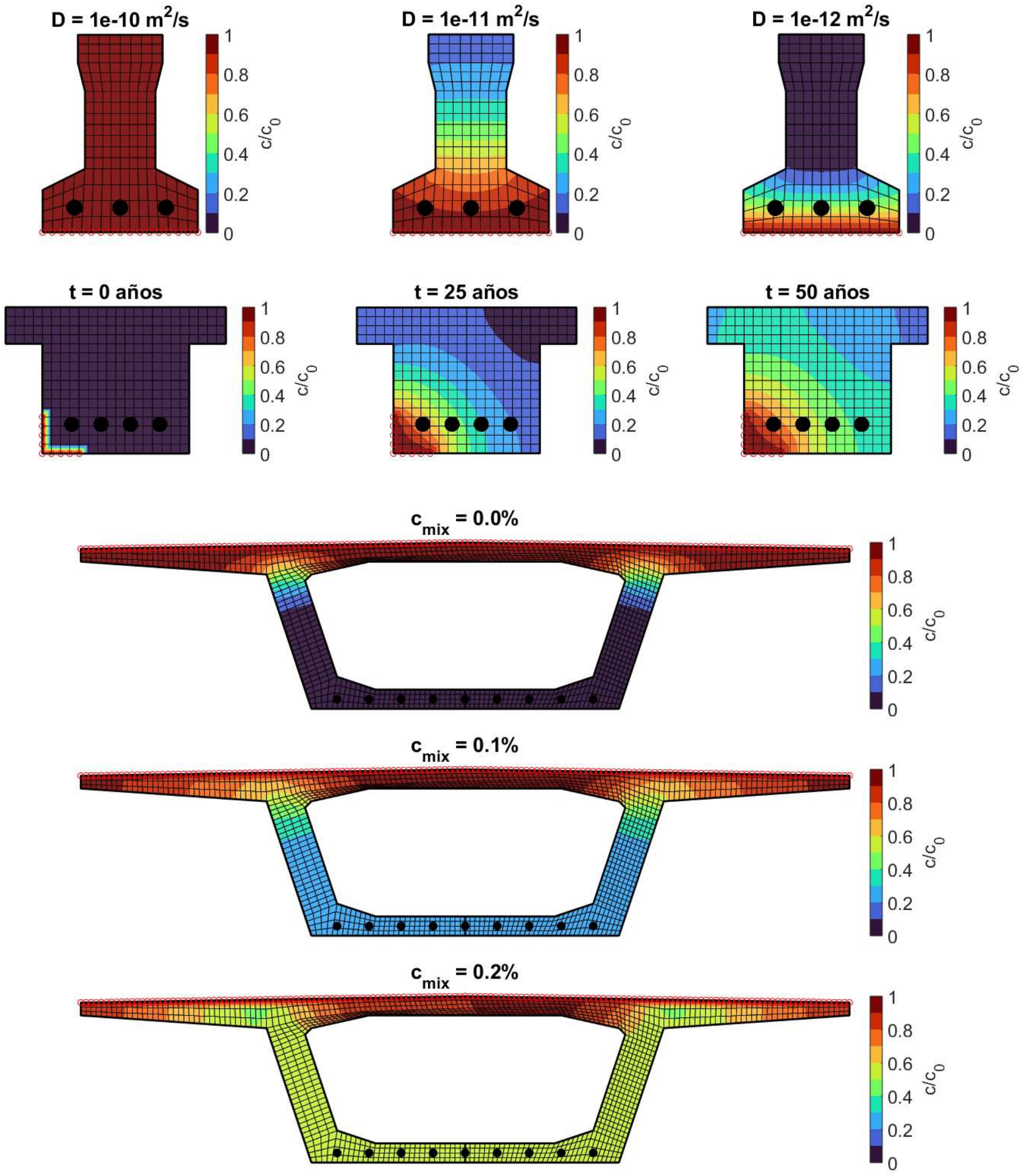

Figure 1. Diffusion model applied to different cross-sections under different parameters and initial conditions.

4.1 Damage variable

The model employs a scalar damage parameter δ, ranging between 0 (undamaged) and 1 (fully damaged), to quantify the extent of degradation.

The loss of cross-rebar sectional area is computed estimated using through the damage variable as:

$$A_{s,r} = (1-\delta)\mathrm{A_{s,0}} \tag{5}$$

Where $A_{s,r}$ is the reduced area, and $A_{s,0}$ is the initial area of reinforcement.

Substituting the cross-sectional areas for circular reinforcement bars, the damage index can also be expressed in terms of the bar diameters:

$$\delta = 1-\left(\frac{\phi_r}{\phi_0}\right)^2 \tag{6}$$

According to [3], the reduced diameter ϕ_r can be found as a function of the original diameter ϕ_0 and the corrosion penetration depth P_x:

$$\phi_r = \phi_0 - \alpha P_x \tag{7}$$

Where α is a parameter controlling the type of attack. In the case of uniform corrosion, α = 2, and for pitting corrosion, 5 ≤ α ≤ 10 [3]. Fig. 2 shows the resulting time evolution of the damage variable for uniform and pitting corrosion.

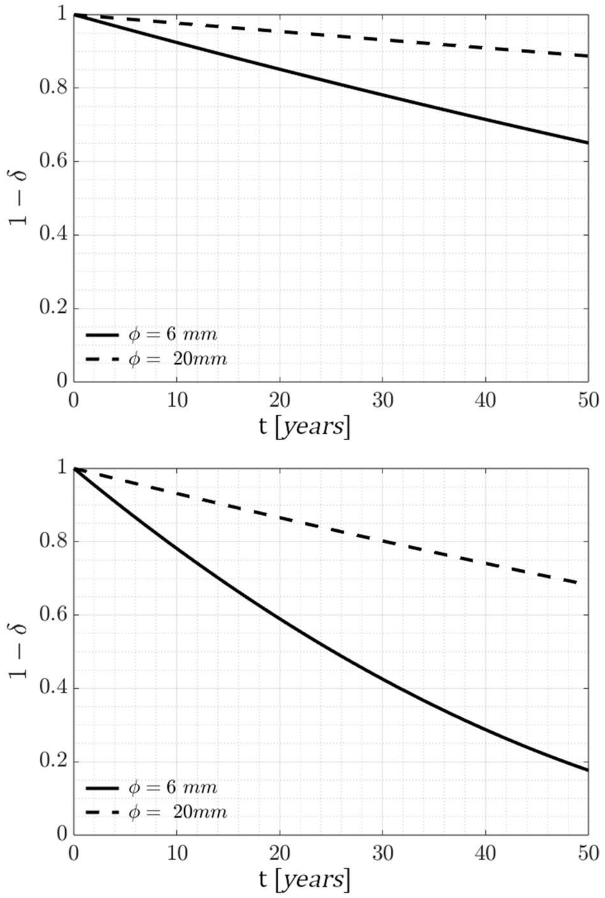

Figure 2. Cross sectional reduction under a current density of 1 μA/cm² for uniform corrosion (α=2) and pitting corrosion (α=6).

The penetration index P_x is related to the corrosion rate v_{corr} and the propagation time t_p by the equation:

$$P_x = v_{corr} t_p \tag{8}$$

There are two ways to establish the value of the corrosion rate: (i) constant, based on the environment, and (ii) continuous, depending on environmental conditions and the characteristics of the concrete.

Prefixed time-invariant values of the corrosion rate can be found in national and international codes depending on the environmental conditions. However, a realistic approach is considered here, where the corrosion rate varies with time, as a result of the diffusion analysis. Therefore, expressed in a continuous form, the corrosion penetration is given by:

$$P_x = \int_{t_0}^{t} v_{corr}(\tau)\, \mathrm{d}\tau \tag{9}$$

To obtain the corrosion rate, the Faraday's Law is used to determine the mass loss during an electrochemical process:

$$\frac{\mathrm{d}m}{\mathrm{d}t} = \frac{M}{nF} I(t) \tag{10}$$

Where *I(t)* is the current intensity, M is the molar mass, *n* it's metal's oxidation number, and F=96,458 °C/mol is the Faraday's constant.

Expressing and developing the mass loss and the current intensity per cross-sectional area, a common relation can be stablished between the corrosion current density and the corrosion velocity:

$$1\, \mu A/cm^2 = 0.0116\, mm/year \tag{11}$$

This relation is used to compute the corrosion velocity needed to determine the penetration index at each time step. In the literature [5], various empirical formulations can be found that relate the corrosion current density to environmental parameters and concrete quality. In the present paper, the formulation found in [6] is used, which establishes the relation shown in Eq. (12) among the current density (μA/cm^2) and the chloride concentration (%kg_{CL}/kg_{Cem}) for environment with humidity below 60%:

$$i_{corr} = 0.0692e^{1.6948Cl} \quad (12)$$

Thus, the procedure to obtain the damage index controlling the structural of corrosion with the diffusion model is described. In summary, for each rebar defined in the cross-section:

1. At each time step k, the chloride concentration from the diffusion model is used to calculate the corresponding current density.

2. From the relationship derived from Faraday's Law, the corrosion rate is determined.

3. The accumulated penetration P_x is calculated. The integral is solved discretely as $P_{x,k} = P_{x,k-1} + \Delta t \cdot v_{corr,k}$.

4. With the corrosion penetration and depending on the attack type, the damage index δ can be obtained for each rebar.

4.2 Effects on the mechanical properties of steel

The damage in the reinforcing steel is considered in two aspects. Firstly, the loss of effective steel area, as described in the previous section, and obtained in the model through Eq. *(5)*. On the other hand, corrosion impacts the mechanical properties of reinforcement steel, including:

1. **Ductility:** Corrosion reduces the elongation capacity of steel under stress, limiting its ability to redistribute forces. In [7], the formulation applied in this model can be found, which is depicted in Fig. 3.

2. **Yield capacity:** Some experimental data suggests a negligible decline in yield strength proportional to corrosion levels, attributed to pitting and surface irregularities. This degradation is difficult to disassociate from the damage in the effective area. To isolate the effect in the material, the detailed geometry of the pits and stress-concentration is needed. Studies in this respect can be found, for example, in [8, 9]. Nevertheless, in the current implementation, the formulation of [7] was used (Fig. 3 – below). This assumption implies that the effect in the yielding stress is minor, although, it can easily be modified in future versions of the model here presented.

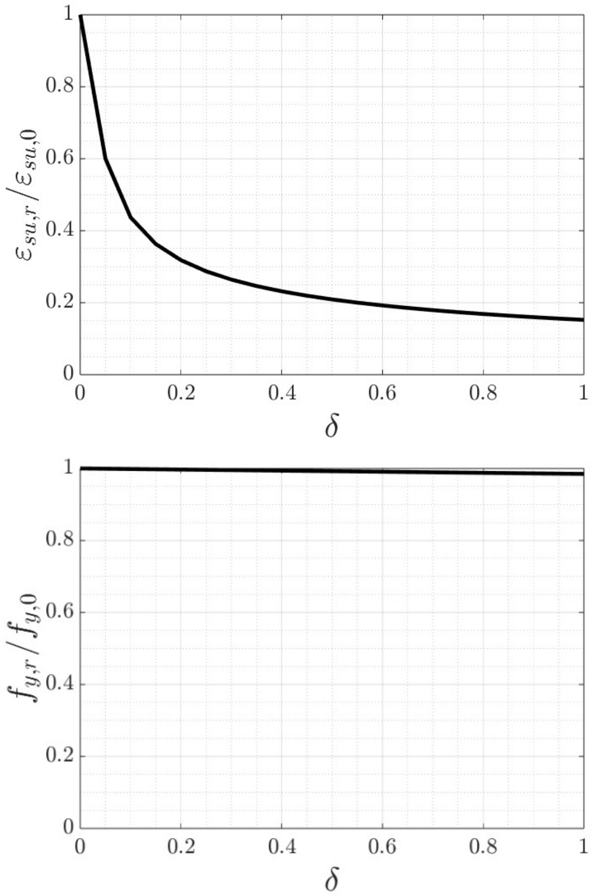

Figure 3. Ductility (above) and yield strength (below) degradation as a function of the index damage.

4.3 Concrete damage

Concrete damage originates primarily from the accumulation of corrosion products at the steel-concrete interface. As the density of the corrosion products is smaller than the steel reinforcement, volumetric expansion is produced inducing radial tensile stresses that manifest as cracking when the tensile strength of the concrete is exceeded. When tension cracks increase, softening of the compression strength take place and, over time, spalling of the protective concrete cover originates.

This degradation can be considered as a reduction of the effective area of the concrete fibre [10], as shown in Eq. (13). This is equivalent to a damage mechanics interpretation.

$$A_c(\delta) = [1 - g(\delta)]A_{c0} \tag{13}$$

Where $A_{c,0}$ is the area of the undamaged concrete fibre, and $g(\delta)$ is the concrete damage parameter as a function of the damage index δ. The concrete damage parameter is computed as in Eq. (14). Where ε_{11} is the average lateral tensile strain, related to the width of the corrosion cracks.

$$g(\delta) = 1 - \frac{1}{1+\kappa\frac{\varepsilon_{11}(\delta)}{\varepsilon_0}}. \tag{14}$$

Finally, there is only left to determine which cross section elements this damage will be applied. Since the cracking begins from the steal-concrete interface towards the concrete free surface, it is applied to the concrete cover around the rebar. According to [7], this approach allows to represent different spalling mechanisms.

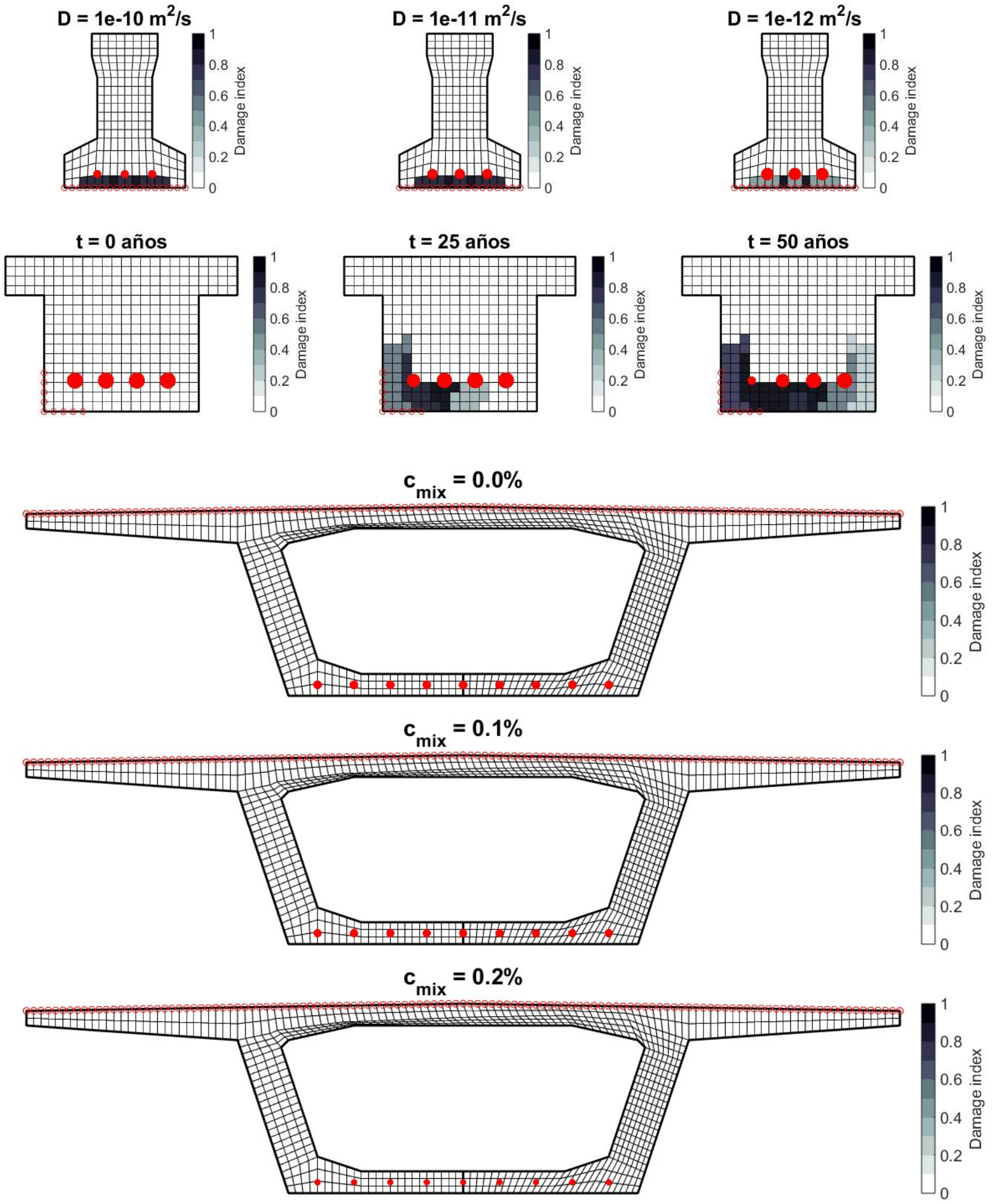

Figure 4. Damage model applied to different cross-sections under different parameters and initial conditions.

5. Application

5.1 Model parameters

Each sub model formerly mentioned includes critical parameters that significantly influence the model's accuracy and predictive capability.

These parameters are summarized in Table 1. In previous sections, the significance of each parameter has been explained or shown graphically.

5.2 Implementation

The implementation of the global model combines the individual components developed in previous sections, integrating them into a unified framework capable of evaluating the structural behavior of reinforced concrete sections subjected to corrosion. The selected approach follows a modular scheme, where each subroutine corresponds to a specific model component: diffusion, damage, and mechanical response.

1. **Diffusion Module**: Calculates the progression of aggressive agents, such as chlorides, within the concrete matrix over time.
2. **Damage Module**: Translates the results from the diffusion module into material and geometric degradation, providing input for the mechanical model by updating the properties of the materials.
3. **Mechanical Model:** computes the structural response of the section under various load conditions using a fiber-based analysis taking into consideration the modified properties due to the outcomes from the damage model.

The interaction between these components is iterative. The output of one module serves as input for the next, ensuring consistency and accuracy in the predictions. To facilitate the computational process, the model was implemented in MATLAB, which is a high-level programming language, supporting parallel computations to handle the complex and resource-intensive calculations efficiently.

5.3 Example

To demonstrate the capabilities of the developed model, the deterioration of moment resistant capacity of the beam shown in Fig. 5-middle will be analyzed.

Table 1. Global model parameters.

	Variable	Símbolo	Uds
Geommetry	Domain vertices	(y, z)	[mm]
	Domain maximum size	h	[mm]
Diffusion	Time	t	[years]
	Diffusion coefficient	D	[mm^2/year]
	Environment concentration	c_0	[kg_{Cl}/kg_{Conc}]
	Initial mix concetration	c_{mix}	[kg_{Cl}/kg_{Conc}]
Damage	Uniform / Pitting	α	[-]
Sectional analysis	Compression strength	f_c	[MPa]
	Yield limit	f_y	[MPa]
	Rebar position	(y_s, z_s)	[mm]
	Rebar diameter	Φ	[mm]

The case-study is an element with a rectangular cross-section with height $h = 500\,mm$ and width $b = 300\,mm$. The considered concrete had a characteristic strength is $f_{ck} = 30MPa$, diffusion coefficient $D = 1 \times 10^{-1}\ \frac{m^2}{s}$. The reinforcement consisted on 2 symmetrical layers of $5\phi 20$ of steel class 500C ($f_{yk} = 500\ MPa$).

As depicted in Fig. 5-top, the element is subjected to an initial chloride concentration of $0.4\%\ \frac{kg_{Cl}}{kg_{Conc}}$ in the bottom left corner. This situation is representative of partially exposed elements due, for instance, to airborne transport. The evolution of the chloride concentration with time is shown in Fig. 5-top, from 0 to 60 years. The concentration affects the bottom reinforcement layers asymmetrically.

Concrete damage initiates in the bottom left corner, as is evidenced in Fig. 5-middle, at 20 years. The propagation of damage in concrete up to 60 years of exposition is indicated in the same figure by means of the evolution of distribution of the damage index. Note the total damage of the concrete in the bottom cover greater deterioration of in the bottom cover in the surroundings of the two rebars in the left edge, which can be predicted by the detailed diffusion model.

The time evolution of the element capacity is shown in Fig. 5-bottom through the moment-curvatures at times 0, 20, 40 and 60 years. It is evidenced that the element not only reduces its moment bearing capacity, but also the ductility is also affected. However, as the resulting effect is less than in the case of uniform damage assumption.

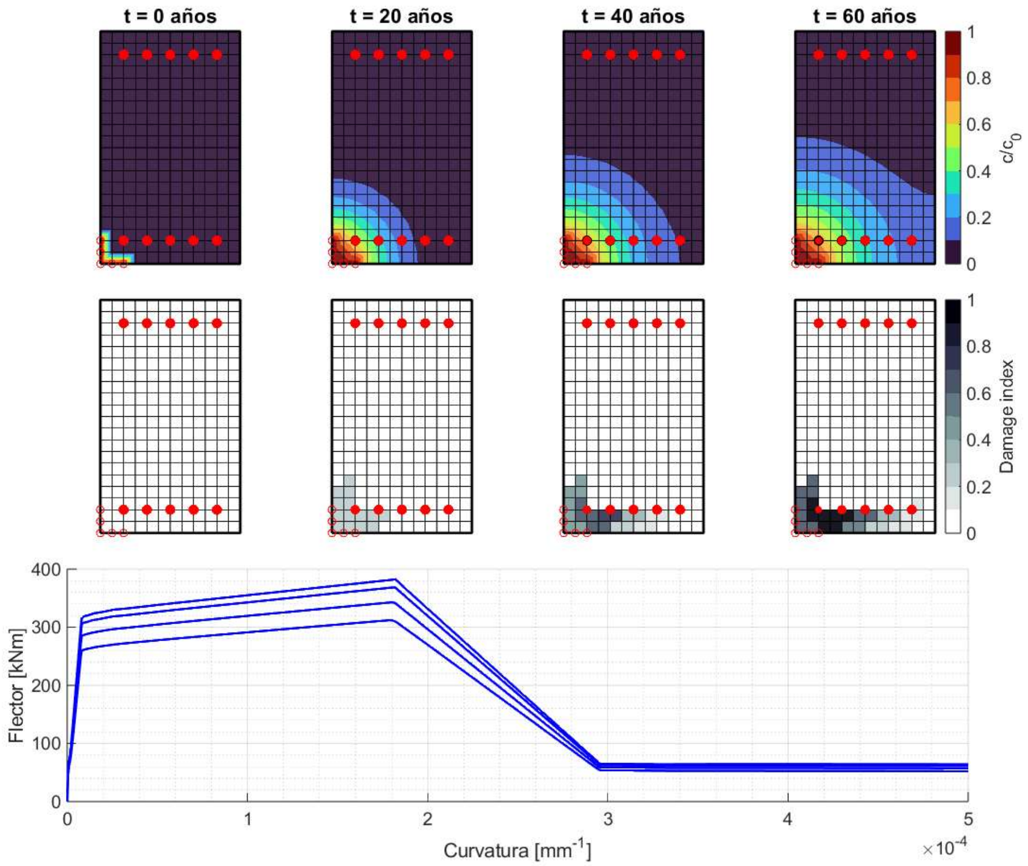

Figure 5. Example of the deterioration model output of a rectangular cross section.

6. Conclusions

A numerical model has been developed which is capable of obtaining the local damage distribution due to corrosion damage of concrete cross-sections. The model framework uses three interacting modules, which analyses the local time-space distribution of the diffusion of corroding agents, the material damage and the resulting degradation of the bearing and deformation capacity for any arbitrary geometry and concentration of chlorides or carbonation. Therefore, the analysis can predict non-uniform damage intensities in the concrete fibers and reinforcing bars in the cross-section and more detailed degradation of the structural capacity.

Acknowledgements

This research has been developed with the the support of research projects PID2021-123701OB-C21, funded by MCIN/ AEI/10.13039/501100011033 and European Regional Development Funds (ERDF) "A way to make Europe", and TED2021-130272B-C21 funded by MCIN/ AEI/10.13039/501100011033 "European Union NextGenerationEU/PRTR".

References

[1] Bowman E, Jacobson G, Koch G, Varney J, Thopson N, Moghissi O, et al. International Measures of Prevention, Application, and Economics of Corrosion Technologies Study. 2016.

[2] Pacheco-Torgal F, Melchers RE, Shi X, De Belie N, Van Tittelboom K, Sáez A. Eco-efficient Repair and Rehabilitation of Concrete Infrastructures. Eco-Efficient Repair Rehabil Concr Infrastructures 2018:1–757. https://doi.org/10.1016/c2016-0-04100-1.

[3] J. Rodriguez and C. Andrade, CONTECVET - A validated Users Manual for assessing the residual service life of concrete structures, Instituto Eduardo Torroja, 2002.

[4] J. Rodriguez, "El Eurocódigo 2 y la evaluación de estructuras de hormigón armado con armaduras corroídas," *Hormigón y Acero,* vol. 65, no. 272, pp. 123-132, 2014.

[5] Y. Liu and R. Meyers, "Modeling the Time-to-Corrosion Cracking in Chloride Contaminated Reinforced Concrete Structures," *ACI Materials Journal,* vol. 95, no. 6, 1998.

[6] W.-Y. Jung, Y.-S. Yoon and Y.-M. Sohn, "Predicting the remaining service life of land concrete by steel corrosion," *Cement and Concrete Research,* vol. 33, no. 5, pp. 663-677, 2003.

[7] F. Biondini and M. Vergani, "Damage modeling and nonlinear analysis of concrete bridges under corrosion," in *Bridge Maintenance, Safety, Management, Resilience and Sustainability*, 2012, pp. 949-957.

[8] I. Fernandez, J.M. Bairán, A. Marí, "Mechanical model to evaluate steel reinforcement corrosion effects on $\sigma - \varepsilon$ and fatigue curves. Experimental calibration and validation", *Engineering Structures*, Vol. 118, 2016, pp. 320-333, doi: 10.1016/j.engstruct.2016.03.055

[9] I. Fernandez, J.M. Bairán, A. Marí, "3D FEM model development from 3D optical measurement technique applied to corroded steel bars", *Construction and Building Materials*, Vol. 124, 2016, pp. 519-532, doi: 10.1016/j.conbuildmat.2016.07.133.

[10] D. Coronelli and P. Gambarova, "Structural Assessment of Corroded Reinforced Concrete Beams: Modeling Guidelines," Journal of Structural Engineering, vol. 130, no. 8, pp. 1214-1224, 2004.